Cyclic Behaviour of Soils and Liquefaction Phenomena, Triantafyllidis (ed)
© 2004 Taylor & Francis Group, London, ISBN 90 5809 620 3

Vibratory driven pile performances in Flanders clay. International Prediction Event 2003

M.T. Ma & A.E. Holeyman
Université Catholique de Louvain, Belgium

ABSTRACT: To address the questions of drivability and load bearing behavior of piles vibratory driven into stiff Flanders clay and how they compare with impact driven piles under same geotechnical condition, instrumented pile tests were conducted at a Flanders clay site in Merville, North France, in April through June of 2003. Measurements of drivability parameters and static load tests were made during vibratory and impact pile tests. Prediction Event 2003 was organized in March of 2003. The differences between the measured results of vibratory and impact driven piles are highlighted, comparisons of measured and predicted results are made.

1 INTRODUCTION

Up until recently, no full-scale test data were available for the drivability and load bearing behavior of vibratory driven pile in Flanders clay. As a part of the French National Vibratory Driving program (Projet National Vibrofonçage), vibratory driven pile tests were carried out at a Flanders clay site in Merville, France, in April through June of 2003. Institut pour la Recherche par Experimentation (IREX) is the Program Manager. Pile driving, instrumentation and testing were performed by French Laboratoire Central des Ponts et Chaussées (LCPC).

Université Catholique de Louvain (UCL), acting as an independent body, organized the Vibratory Driven Pile Performances in Flanders Clay International Prediction Event 2003, a Class A prediction event. In March 2003, invitations to submit predictions were extended to geotechnical engineers around the globe. Predictions were received in April and May of 2003.

2 SOIL INVESTIGATION

At the Merville site, the soil is silt from 0 to 2.2 m. It has a Menard limit pressure of 0.25 to 0.6 MPa and a cone penetration resistance of 1 MPa. From 2.2 to 42 m, Flanders clay is found. The Menard limit pressure in this layer increases with depth from 0.75 MPa at 4 m and 1.8 Mpa at 16 m. The cone resistances are 2 MPa at 4 m and 5 MPa at 16 m. Below 42 m, the soil is composed of sand and Landenian clay. At 10 m where the test piles were expected to reach, Menard limit pressure is 1.25 MPa, CPT resistance is 2.50 MPa and SPT blow counts is 20, indicating that the Flanders clay is stiff.

3 TEST PILE INSTALLATION

The pile group that was to be vibratory driven, consisted of one double AU16 sheet pile (sheet pile thereafter) and one open ended 508 mm diameter pipe pile (pipe pile thereafter). Identical piles, installed in the same area, were to be impact driven (Figure 1). The pile charateristics are shown in Table 1. Model ICE 815 vibrator was used for vibratory driving. Model IHC S70 hammer was used for impact driving.

The sheet pile was vibratory driven to 6.95 m, depth of refusal. An identical sheet pile was then impact driven to the same depth. Similarly, a pipe pile was vibratory driven to 9.40 m, followed by another pipe pile, impact driven to 9.40 m. The scheme was

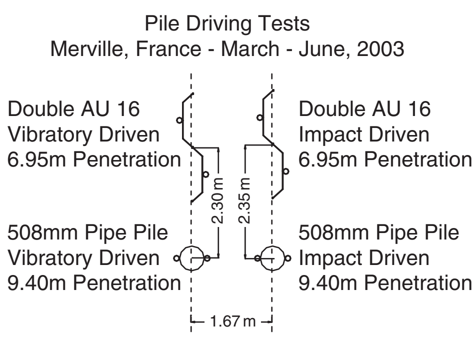

Figure 1. Pile arrangement.

Table 1. Pile characteristics.

Type of pile	Length (m)	Weight (kg/m)	Section (cm^2)
Dbl AU 16	13.01	167.0	212.7
508 mm Ø	12.37	182.35	232.33

designed to allow direct comparison of the vibratory and impact drivabilities of the sheet pile and the pipe pile, their static load bearing behaviors and ground vibration intensities incurred. The pipe piles were plugged during driving.

4 PREDICTIONS

13 predictions were received. Names and affiliations of the predictors are not identified.

Prediction 1

Predictor applied API RP2A method to compute bearing capacity. Load vs. settlement curves were obtained by use of side shear and end bearing transfer functions proposed by Everett (1991).

Prediction 2

The wave equation program GRLWEAP was used to evaluate the pile drivability. The input parameters were lengths of elements, sections, modulus of elasticity, maximum resistance of each element, quake and damping coefficients. Semple and Gemeinhardt (1981) method was used to assess the load-settlement behavior.

Prediction 3

GRLWEAP: Speed of penetration and blows per minute were computed for vibratory and impact driven sheet piles by this program.

Hypervib II: This is a 1-D concentric ring, constitutive model where the rigid pile is surrounded by rigid concentric soil rings with mass and springs that transfer shear forces to neighboring rings by dynamic shear equilibrium. The displacement was computed by numerical integration of equation of motion. The shear stresses between pile shaft and soil and between soil rings followed the pattern of hysteretic loops that were functions of pile-soil and soil-soil displacements. The toe resistance was simulated by a spring-dashpot. A slider mechanism was used at the toe to assign zero resistance when pile moves up. The input parameters of the model were derived from CPT tests.

Vitpene: Plastic soil and rigid pile are assumed in this model. All drivability quantities are computed by numerical integration of equations of motion.

Prediction 4

TNOWAVE, a Smith type 1-D stress wave pile driving analysis program, was used to predict the vibratory and impact drivabilities.

Prediction 5

Predictor used his own proprietary program and research data to prepare the impact drivability prediction. Load bearing capacities were computed using Myerhof formulae.

Prediction 6

Load-settlement behavior prediction was based on Dyka's PhD thesis (2001) which used a hybrid plastic model to predict the limit resistance. The shaft load transfer functions were based on solutions by Randolph and Wroth (1978). The load vs. settlement behavior at the pile toe followed Boussinesq formula. Van Impe–De Clercq and Gwizdala-Tejchman hyperbolic curves were used to describe shear modulus variation with shear strain.

Prediction 7

Predictor used his own Smith type, 1-D wave equation analysis program to make the vibratory and impact drivability predictions.

Prediction 8

The soil resistance was computed using procedures by Stevens, Wiltsie and Turton (1982) for an unplugged pile. The shear strength of clay was determined from the CPT data. The pile capacity was computed by API method. Drivability analysis was performed by GRLWEAP.

Prediction 9

Skin and toe unit resistances were derived from the CPT data. The ultimate point resistance was obtained by De Beer method. The skin friction degradation at large deformation was considered. The load vs. settlement curve was plotted following a plasto-elastic, hyperbolic function.

Prediction 10

End bearing capacity was evaluated by a slip-line field method in which end bearing capacity was influenced by neighboring skin friction stress. The limit skin friction stress was obtained by Bruland's effective stress model. Load-settlement curves were obtained by use of a load-transfer theory in which stresses at the soil/pile interface is proportional to the settlement at small displacement.

Prediction 11

API RP 2A and Kolk & Van der Velde methods were used to prepare the load bearing behavior.

Prediction 12

Plaxis, a finite element analysis program was used to obtain the ultimate pile base and shaft resistances. Chin's method was used to evaluate the bearing capacity and load vs. settlement curves.

Prediction 13

For load capacity prediction, three methods: Bustamente, Tomlinsom, Togliani, were used and results were compared. Mayne and Schneider method was used to predict load vs. settlement behavior.

5 MERVILLE PILE TEST RESULTS

For vibratory driven sheet pile, accelerations, stresses at top and bottom of piles, suspension forces, Peak

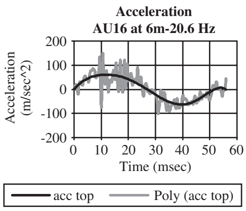

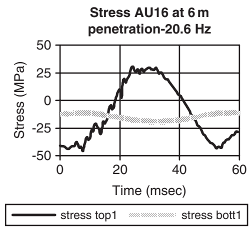

Figure 2. Accelerations of vibratory driven sheet pile.

Figure 3. Stress of vibratory driven sheet pile.

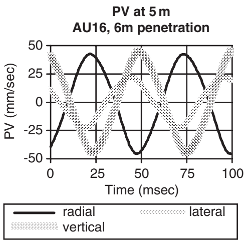

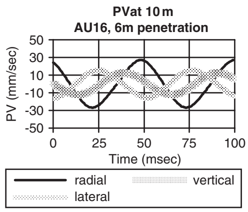

Figure 4. PVs at 5 m.

Figure 5. PVs at 10 m.

Particle Velocity (PV) at 5, 10, 15 m from pile, load vs. settlement behavior, penetration log and ultimate load were measured continuously from start to depth of refusal at 6.95 m. Data graphs at 6 m penetration are shown below as examples. Some data recorded were abnormal and are not shown.

Figure 2 shows the acceleration at top of sheet pile. Figure 3 shows that the top and bottom stresses have a phase angle shift and a difference in amplitude. The sheet pile section is anti-symmetrical with respect to both axes. It also has a weak torsional rigidity, especially at shallow penetration where restraint from surrounding soil is minimum. Its dynamic responses were 3 dimensional, therefore, the stresses at various locations were different. The amplitudes of the stresses at the bottom are smaller because as pile penetrates, it mobilizes soil resistance that opposes the driving stresses.

Figures 4, 5, 6 depict the peak particle velocities (PVs) at 5, 10, 15 m from pile when penetration reached 6 m. The amplitudes of the PVs in radial, lateral and vertical directions attenuate as the distance from the source increases. The suspension force variation in 1500 msec is shown in Figure 7.

When ultimate capacity is reached (Figure 8), a small increase in load is accompanied by a large increase in settlement. This is caused by soil strain hardening under vibratory shearing strain.

Measurements of accelerations, stresses, particle velocities and load vs. settlement curves for impact driven pipe pile are presented below. Differences between the vibratory and impact driving measurements are highlighted.

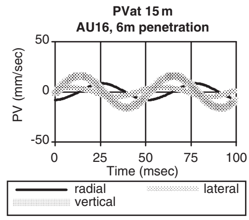

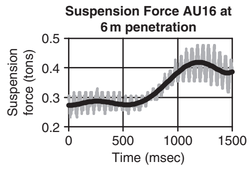

Figure 6. PVs at 15 m.

Figure 7. Suspension force.

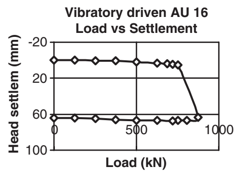

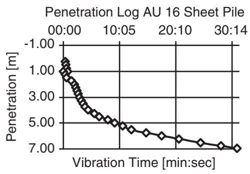

Figure 8. Load vs. settlement.

Figure 9. Penetration log.

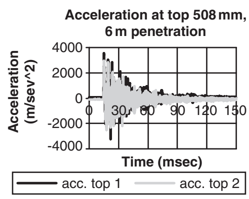

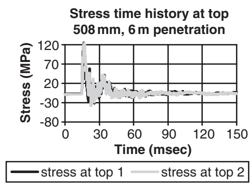

Figure 10. Acceleration of impact driven pipe pile.

Figure 11. Stress at top of impact driven pipe pile.

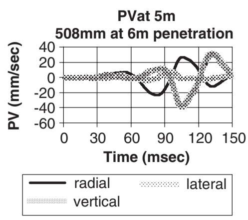

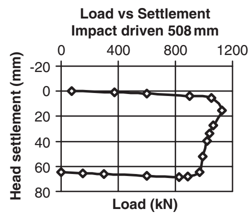

Figure 12. PVs at 6 m.

Figure 13. Load vs. settlement impact driven pipe pile.

The high frequency spikes from impact driving on the acceleration graphs reached 3600 m/sec^2 (Figure 10). However, these local spikes have little influence on the overall speed of penetration.

The P, S, and Rayleigh waves can be identified from the above PV graphs at 5 m from pile (Figure 12). PVs incurred by impact driving are in the order of 30 mm/sec. This compared with the PVs of 44 mm/sec by vibratory driving.

As opposed to vibratory driving, an increase of settlement beyond ultimate load was accompanied by a decrease of load when the soil was softened by impact driving (Figure 13).

6 COMPARISONS OF PREDICTIONS AND MEASURMENTS

Wherever possible, diverse prediction formats received were adjusted to conform with test format.

The comparison graphs are presented in sequence of acceleration, stress, enthru, blow counts, PVs, speed of penetration, load vs. settlement, and ultimate load bearing capacity.

Accelerations of Prediction 3 (P3) were based on rigid pile model. The accelerations at the top and bottom of pile are the same by definition. P4 used an elastic pile model.

In test, maximum and minimum stresses were measured at the top and bottom of pile. The Prediction 3 (Pred 3) stresses (Figure 15) were based on rigid pile model. Pred 5 did not specify maximum and minimum stresses.

In Pred 3, enthru increases gradually with depth of penetration (Figure 16). The enthru steps in Pred 8 are similar to as tested between 3 m and 9 m depths of penetration.

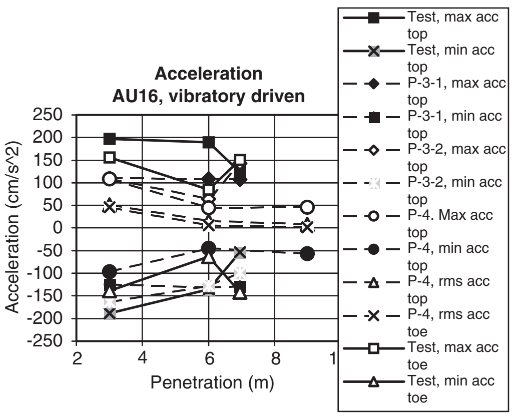

Figure 14. Acceleration of vibratory driven sheet pile.

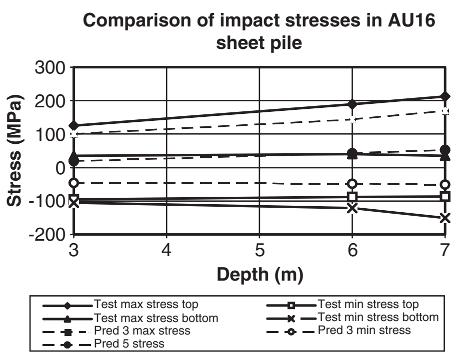

Figure 15. Stress of vibratory driven sheet pile.

Pred 8's blow counts per 25 cm penetration for pipe pile (Figure 17), shows good agreement with tested values.

Tested PVs included three directions: radial, lateral and vertical (Figure 18). Comparison of tested and predicted PVs shows that the art of accurately predicting PVs remains elusive.

The predicted speed of penetrations are considerably higher than the tested (Figure 19).

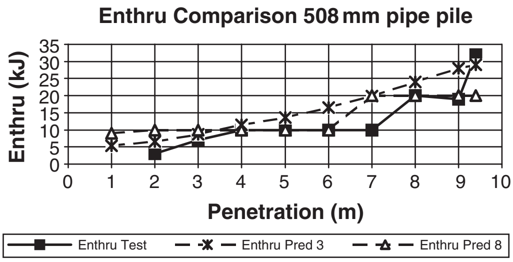

Figure 16. Enthru of impact driven pipe pile.

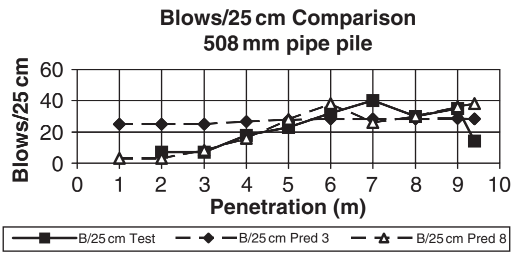

Figure 17. Blows/25 cm of pipe pile.

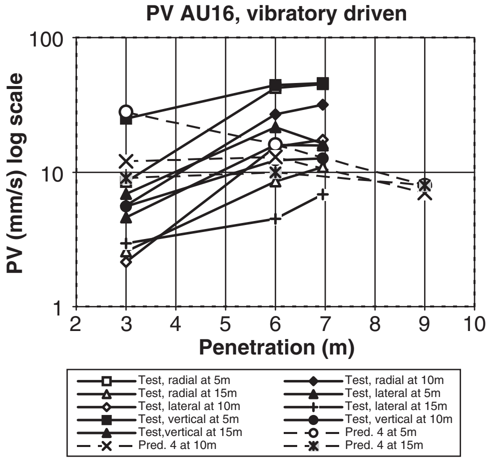

Figure 18. PVs of vibratory driven sheet pile.

Load vs. settlement behavior predicted by Pred 1 and Pred 6 are in fairly good agreement with tested (Figure 20).

The predicted ultimate loads (Figure 21) came in various formats. To determine the ultimate loads we used somewhat arbitrarily, one of four methods below:

1. Ultimate loads as stated by the Predictors.
2. Pile head settlement corresponding to 10% of the pile diameter.
3. Ultimate point about which settlement curve, rotates abruptly downward.

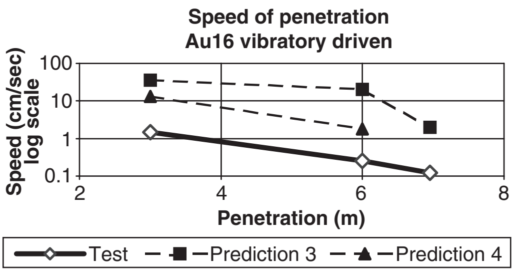

Figure 19. Speed of Penetration of vibratory driven sheet pile.

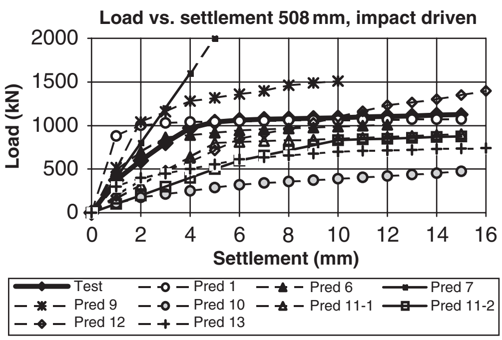

Figure 20. Load vs. settlement.

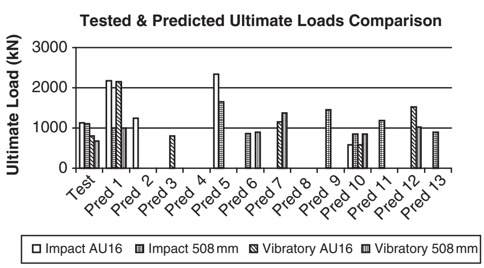

Figure 21. Ultimate Loads, for sheet and pipe piles, vibratory & impact driven.

4. Loads on the load vs. penetration curve pecked at 9.4 m penetration where impact driving stopped or at 6.95 m where vibratory driving met refusal.

Predictions 1, 10, 12 show identical values for impact and vibratory driven piles. These occur when Predictors did not specify the method of driving. The wide range of predicted ultimate loads clearly indicates the difficulty of modeling the soil-pile interaction.

7 CONCLUSION

- 1D concentric ring, constitutive model yielded reasonable acceleration predictions for vibratory driven sheet pile. (Prediction 3)
- 1D Smith type GRLWEAP computed stress levels comparable to tested. (Prediction 3)
- Load vs. settlement behavior predicted by Everett method and a composite of CPT data, Polish Code, API was in good agreement with tested. (Prediction 1, Prediction 6)
- Enthru and blow/25 cm predicted by using GRLWEAP gave satisfactory results. (Prediction 8)
- Piles can be vibratory driven into Flanders clay to limited depth.
- Prediction of speed of penetration remains difficult.
- Tests show lower ultimate capacities for vibratory driven piles than impact driven piles.
- Predicted ultimate capacities are substantially different than tested capacities. The main reasons are the difficulty of modeling complex soil – pile interaction and lack of uniform standards to allow deriving ultimate capacities from load vs. pile settlement curve.
- Accurate PV prediction remains elusive.

REFERENCES

Amar S. et Jézéquel J-F. (1972). Essais en place et en laboratoire sur sols cohérents- Comparaison des résultats, Bulletin des LPC N° 58, pp. 97–108.

Baguelin F., Jézéquel J-F & Shields D.H. (1978). The pressuremeter and foundation engineering, Series on rock and soil mechanics, Vol. 2, N° 4, 1st edition, Transtech publications, Germany.

Benali A. (2002). Semi-empirical analysis of the bearing capacity of single piles, Post-Graduation dissertation (Magister), Departement of Civil Engineering, University of Blida.

Borel S. (2000). Caractéristiques géotechniques du site de Merville (Nord France)

Borel S. & LaCoste F.R. (2002). Plot d'essai de Merville (Nord, France).

Bouafia A. & Benali A. (2003). CPT-based method of bearing capacity of driven piles in clays, Computers and Geotechnics (in progress).

Burland J.B. (1973). Shaft friction piles in clay – A simple fundamental approach. Ground Engineering, Vol. 6, N° 3, pp. 30–42.

Canépa Y., Borel S. & Deconinck J. (2002). Détermination de la courbe d'évolution du module de cisaillement d'un sol en fonction de sa déformation à partir d'essais en place, Compte-rendus du Symposium International Identification et détermination des paramètres des sols et des roches pour les calculs géotechniques PARAM 2002, LCPC, pp. 25–32.

Dyka I. (2001). The analysis and the calculation method of pile group settlement. PhD thesis (in Polish), Technical University of Gdansk.

Ferber V. & Abraham O. (2003). Apport des méthodes sismiques pour la détermination des modules élastiques initiaux: application au site expérimental de Merville, Compterendus du Symposium International Identification et détermination des paramètres des sols et des roches pour les calculs géotechniques PARAM 2002, LCPC, pp. 41–48.

Guédon dubied S. (2003) Résultat des essais par Microscopie Electronique à Balayage, 1 page 18 planches.

Mayne P.W. & Rix G.J. (1993). "G_{max}-q_c Relationships for Clays". Geotechnical Testing Journal, 16(1) 1993, pp. 54–60.

Mengé P. (2001). Soil investigation results at Sint-Katelijne-

Platret G. & Plantet A. (2002). Résultat des essais par diffractométrie aux rayons X, 7 pages, 6 planches.

Poulos H.G. (1989). Pile behaviour- Theory and application, 29th Rankine Lecture, Géotechnique39, N° 3, pp. 365–415.

Tejchman A., Gwizdala K. & Dyka I. (2001). "Analysis of settlements of piled foundations" submitted for the Proceedings 15-th International Conference on Soil Mechanics and Foundation Engineering, Istanbul, Turkey, 2001.

Terzaghi K., Peck R. & Mesrif G. (1996). Soil mechanics in engineering practice, John Wiley & Sons. Third edition.

Waver (Belgium), Screw Piles – installation and design in stiff clay, Holeyman Editor, Balkema, pp. 19–62.

Yaich-Achour N. (2003). Paramètres de transfert de charges des fondations profondes- Analyse d'une banque de Données (in French), Post-Graduation dissertation (Magister), Departement of Civil Engineering, Universityof Blida.